Dynamical Density Functional Theory with Hydrodynamic Interactions and Colloids in Unstable Traps

M. Rex* and H. Löwen

Institut für Theoretische Physik II: Weiche Materie, Heinrich-Heine-Universität Düsseldorf, Universitätsstraße 1, D-40225 Düsseldorf, Germany

(Received 13 March 2008; published 29 September 2008)

A density functional theory for colloidal dynamics is presented which includes hydrodynamic interactions between the colloidal particles. The theory is applied to the dynamics of colloidal particles in an optical trap which switches periodically in time from a stable to an unstable confining potential. In the absence of hydrodynamic interactions, the resulting density breathing mode exhibits huge single peaked oscillations in the trap center which become double peaked and damped by hydrodynamic interactions. The predicted dynamical density fields are in good agreement with Brownian dynamics computer simulations.

DOI: 10.1103/PhysRevLett.101.148302 PACS numbers: 82.70.Dd, 05.70.Ln, 61.20.Gy, 61.20.Ja

The dynamics of mesoscopic colloidal particles dispersed in a molecular solvent is of fundamental importance for an understanding of soft matter transport and flow properties. The control over the collective colloidal dynamics leads to the construction of ''smart'' materials steered by external fields like electro- or magnetorheological fluids [1] and is essential for applications such as gelation and aggregation in paints and cosmetics [2]. Apart from the stochastic Brownian motion of the colloidal particles due to collisions with the solvent molecules, hydrodynamic interactions between colloidal particles arising from the induced solvent flow field are relevant in concentrated suspensions. It has been shown by experiments [3,4], computer simulations [5,6] and theory [7–10] that hydrodynamic interactions can lead to qualitatively different behavior in the bulk transport properties and in colloidal sedimentation [11] as compared to simple Brownian motion valid at very low volume fractions.

The goal of this Letter is twofold. First we construct a dynamical density functional theory which incorporates hydrodynamic interactions. The theory is explicitly worked out for far-field hydrodynamic interactions on the Rotne-Prager level and generalizes earlier formulations [12,13] where hydrodynamic interactions were neglected. The theory makes predictions for an arbitrary time-dependent external potential, i.e., for a general inhomogeneous nonequilibrium situation. Second, we consider the dynamics of colloidal particles confined in an unstable optical trap which switches periodically in time from a stable to unstable confining potential. This situation can in principle be realized, e.g., by combining two laser tweezers or by scanning around a single laser tweezer quickly [3,14,15]. The response to this oscillating trap is a time-dependent radial-symmetric *breathing mode* [16]. Here we show that the breathing mode is tunable by hydrodynamics and is therefore qualitatively different from that of thermally excited trapped Bose gases [16] (where quantum mechanics plays a key role) and that from excited dust Coulomb clusters [17] (where the damping is absent). It is important to unravel the underlying physics of the breathing mode since it can be technologically exploited as an ultrasonic emitter [18].

As a result of our calculations the properties of the breathing mode strongly depend on hydrodynamic interactions. For instance, significant oscillations in the density profile in the trap center which built up if no hydrodynamic interactions are present become double peaked and damped by hydrodynamic interactions. The predictions of the dynamical density functional theory are in very good agreement with Brownian dynamics nonequilibrium computer simulations which take hydrodynamic interactions into account on the same level as the theory does. The theory can also provide a possible route to incorporate hydrodynamic interactions into dynamical approaches like mode-coupling theory [19].

The starting point of the derivation of the dynamical density functional theory including hydrodynamic interactions on the two-body level is the Smoluchowski equation, i.e., the equation for the time evolution of the full probability density distribution $P(\mathbf{r}^N, t)$ for N interacting spherical Brownian particles at positions $\mathbf{r}^N = \mathbf{r}_1, \mathbf{r}_2, ..., \mathbf{r}_N$ and time t:

$$\frac{\partial P(\mathbf{r}^N, t)}{\partial t} = \sum_{i,j}^{N} \nabla_i \cdot \mathbf{D}_{ij}(\mathbf{r}^N) \cdot \left[\nabla_j + \frac{\nabla_j U(\mathbf{r}^N, t)}{k_B T}\right] P(\mathbf{r}^N, t), \tag{1}$$

where $k_B T$ is the thermal energy. We assume pairwise additivity for the total potential energy of the system, such that $U(\mathbf{r}^N, t) = \sum_{k=1}^{N} V_{\text{ext}}(\mathbf{r}_k, t) + \frac{1}{2} \sum_{k=1}^{N} \sum_{l \neq k}^{N} v_2(\mathbf{r}_k, \mathbf{r}_l)$, where $V_{\text{ext}}(\mathbf{r}, t)$ is the one-body time-dependent external potential acting on each particle and $v_2(\mathbf{r}, \mathbf{r}')$ is the pair interaction potential. Hydrodynamic interactions mediated by the flow of moving neighboring particles are included

through the configuration-dependent diffusion tensor—an inverse resistance matrix relating all acting forces to all velocities of the particles—which we approximate on a two particle level: $\mathbf{D}_{ij}(\mathbf{r}^N) \approx D_0\mathbf{1}\delta_{ij} + D_0[\delta_{ij}\sum_{l\neq i}^{N}\boldsymbol{\omega}_{11}(\mathbf{r}_i-\mathbf{r}_l) + (1-\delta_{ij})\boldsymbol{\omega}_{12}(\mathbf{r}_i-\mathbf{r}_j)]$. Here, D_0 denotes the diffusion constant of a single isolated particle. Series expansions of the two tensors $\boldsymbol{\omega}_{11}$ and $\boldsymbol{\omega}_{12}$ are known, in principle, to arbitrary order [20]. By integrating Eq. (1) with $N\int d\mathbf{r}_2 \ldots \int d\mathbf{r}_N$, we obtain the equation for the time evolution of the one-body density $\rho(\mathbf{r}, t)$. The resulting equation depends on both, the time-dependent two-body and the three-body densities. We cast those into a form involving exclusively the equilibrium Helmholtz free energy functional $\mathcal{F}[\rho] = k_BT\int d\mathbf{r}\rho(\mathbf{r}, t)[\ln(\Lambda^3\rho(\mathbf{r}, t)) - 1] + \mathcal{F}_{\text{exc}}[\rho] + \int d\mathbf{r}\rho(\mathbf{r}, t)V_{\text{ext}}(\mathbf{r}, t)$, with $\mathcal{F}_{\text{exc}}[\rho]$ being the excess contribution to the free energy functional and Λ the thermal de Broglie wavelength, by making use of static DFT [21] and the first two members of the Yvon-Born-Green (YBG) relations (see, e.g., [22]). To that end, we identify the out-of-equilibrium system at each point in time with an equilibrium reference system whose density profiles are identical. The basic assumption now, which also underlies the original version of the DDFT [12,13], is to approximate the nonequilibrium two-body and three-body densities by those of the equilibrium reference system. Thus, we obtain our central result:

$$\frac{k_BT}{D_0}\frac{\partial\rho(\mathbf{r},t)}{\partial t} = \nabla_{\mathbf{r}}\cdot\left\{\rho(\mathbf{r},t)\nabla_{\mathbf{r}}\frac{\delta\mathcal{F}[\rho]}{\delta\rho(\mathbf{r},t)} + \int d\mathbf{r}'\rho^{(2)}(\mathbf{r},\mathbf{r}',t)\boldsymbol{\omega}_{11}(\mathbf{r}-\mathbf{r}')\cdot\nabla_{\mathbf{r}}\frac{\delta\mathcal{F}[\rho]}{\delta\rho(\mathbf{r},t)} + \int d\mathbf{r}'\rho^{(2)}(\mathbf{r},\mathbf{r}',t)\boldsymbol{\omega}_{12}(\mathbf{r}-\mathbf{r}')\cdot\nabla_{\mathbf{r}'}\frac{\delta\mathcal{F}[\rho]}{\delta\rho(\mathbf{r}',t)}\right\}. \tag{2}$$

Equation (2) has the form of a continuity equation with the current density $\mathbf{j} = \mathbf{j}_1 + \mathbf{j}_2 + \mathbf{j}_3$ given by the terms in the curly brackets. The current density $\mathbf{j}_1$ is proportional to the thermodynamic force $\nabla_{\mathbf{r}}\frac{\delta\mathcal{F}[\rho]}{\delta\rho(\mathbf{r},t)}$ and persists when hydrodynamic interactions are neglected [13]. $\mathbf{j}_2$ and $\mathbf{j}_3$ are additional current densities which occur due to the solvent mediated hydrodynamic interactions. $\mathbf{j}_2$ describes the current density stemming from the reflection of the solvent flow induced by the thermodynamic force at position $\mathbf{r}$ on the surrounding particles. $\mathbf{j}_3$, on the other hand, is the current density at position $\mathbf{r}$ due to the solvent flow induced by the thermodynamic force at position $\mathbf{r}'$.

Finally, we close the above relation Eq. (2), which still depends on the nonequilibrium two-body density $\rho^{(2)}(\mathbf{r}, \mathbf{r}', t)$. Within our approximation it is given at every point in time by the exact generalized Ornstein-Zernike equation [21]:

$$\rho^{(2)}(\mathbf{r}, \mathbf{r}', t) = (1 + c^{(2)}(\mathbf{r}, \mathbf{r}'))\rho(\mathbf{r}, t)\rho(\mathbf{r}', t) + \rho(\mathbf{r}', t)\int d\mathbf{r}''(\rho^{(2)}(\mathbf{r}, \mathbf{r}'', t) - \rho(\mathbf{r}, t)\rho(\mathbf{r}'', t))c^{(2)}(\mathbf{r}'', \mathbf{r}'), \tag{3}$$

with the Ornstein-Zernike direct correlation function $c^{(2)}(\mathbf{r}, \mathbf{r}') = \frac{\delta^2\mathcal{F}_{\text{exc}}[\rho]}{\delta\rho(\mathbf{r},t)\delta\rho(\mathbf{r}',t)}$. This implicit equation for the two-body density of the inhomogeneous system may be reasonably approximated by its bulk value [23,24], i.e.: $\rho^{(2)}(\mathbf{r}, \mathbf{r}', t) \approx \rho(r, t)\rho(r', t)g(|\mathbf{r} - \mathbf{r}'|, \bar{\rho})$, where $g(|\mathbf{r} - \mathbf{r}'|, \bar{\rho})$ is the pair correlation function for a homogeneous system at an appropriately averaged density $\bar{\rho}$ for which analytic expressions are available [25].

We use the method presented here to investigate the time-evolution of the one-body density of a confined cluster of $N = 100$ monodisperse hard spherical particles of diameter σ, which serves as the unit of length henceforth. An appropriate time scale which also incorporates the solvent viscosity is $\tau_B = \sigma^2/D_0$. The particles are trapped in a soft spherical cavity which switches from a stable to an unstable shape periodically in time. The confining external potential only acts on the colloidal particles while the solvent is treated as an unbounded fluid. The total external potential is modeled as

$$V_{\text{ext}}(r, t) = V_1\left(\frac{r}{R_1}\right)^4 + V_2\cos(2\pi t/\tau)\left(\frac{r}{R_2}\right)^2, \tag{4}$$

where $r = |\mathbf{r}|$, $R_1 = 4\sigma$ and $V_1 = 10k_BT$ are the length scale and the strength of an outer fixed cavity and $R_2 = \sigma$ and $V_2 = k_BT$ are the length scale and strength of an inner part, which oscillates in time with a period $\tau = 0.5\tau_B$. We expect the effect of hydrodynamic interactions to be most prominent for a period in this regime because in the limit of small τ particles barely move and in the other limit for large τ the effect of hydrodynamic interactions should disappear. A sketch of the setup is shown in Fig. 1. Because of the spherical symmetry, the density profile $\rho(r, t)$ depends only on the radial position coordinate r.

For the hard sphere excess density functional $\mathcal{F}_{\text{exc}}[\rho]$ Rosenfeld's fundamental measure theory [26] was used which provides a very reliable approximation in equilibrium [27]. The distinct hydrodynamic tensor $\boldsymbol{\omega}_{12}(\mathbf{r})$ is approximated by the Rotne-Prager expression [28] $\boldsymbol{\omega}_{12}(\mathbf{r}) = \frac{3}{8}(\frac{\sigma_H}{r})[\mathbf{1} + \hat{\mathbf{r}}\,\hat{\mathbf{r}}] + \frac{1}{16}(\frac{\sigma_H}{r})^3[\mathbf{1} - 3\hat{\mathbf{r}}\,\hat{\mathbf{r}}] + \mathcal{O}[(\frac{\sigma_H}{r})^7]$ while the self term $\boldsymbol{\omega}_{11}(\mathbf{r})$ whose leading order term is $\mathcal{O}((\sigma_H/r)^4)$ is neglected. Here, $\hat{\mathbf{r}} = \mathbf{r}/|\mathbf{r}|$ denotes the unit vector, $\hat{\mathbf{r}}\,\hat{\mathbf{r}}$ is the dyadic product, and $\mathbf{1}$ is the unit matrix. In our studies we have chosen the hydrodynamic diameter to be $\sigma_H = 3\sigma/4$. Thus, on this level of approximation, we incorporate all solvent mediated interactions up to order of $\mathcal{O}((\sigma_H/r)^3)$. The pair correlation $g(|\mathbf{r} - \mathbf{r}'|, \bar{\rho})$ is calculated at each time step at the average density of the system

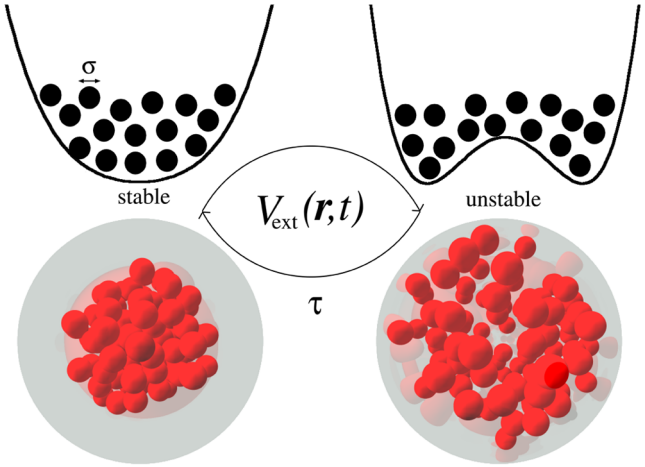

FIG. 1 (color online). Sketch of the confined system. The external potential models an optical trap $V_{ext}(r, t)$ which changes its central shape from stable to unstable within a time period τ. The trap confines N colloidal hard spheres of diameter σ shown as black circles. Additionally, typical $3d$ simulation snapshots are shown. The left-hand side shows an initial stable configuration for $t = 0$ and the right-hand side shows an unstable situation at $t = 2.75\tau_B$ for case (N) [34].

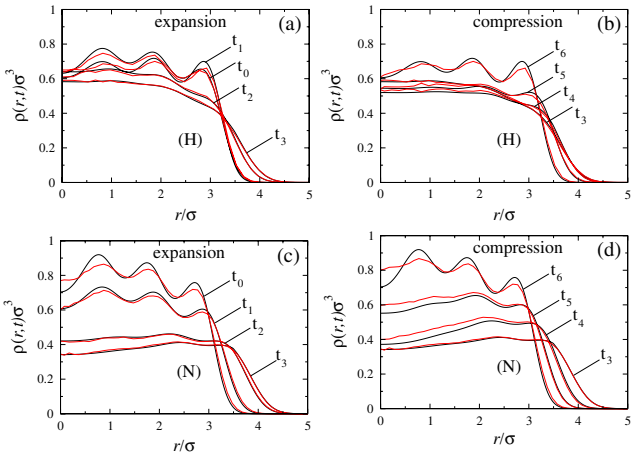

FIG. 2 (color online). *Steady-state* DDFT (solid curves) and BD (noisy curves) results for the time-dependent density profile $\rho(r, t)$. In Fig. (a) and (b) hydrodynamic interactions are taken into account while in (c) and (d) they are neglected. (a) and (c) correspond to the expanding half period and (b) and (d) to the compressing half period, respectively [34]. The profiles correspond to the following time sequence: $t_0 = 2.5\tau_B$, $t_1 = 2.6\tau_B$, $t_2 = 2.7\tau_B$, $t_3 = 2.75\tau_B$ in (a) and (c), and $t_3 = 2.75\tau_B$, $t_4 = 2.85\tau_B$, $t_5 = 2.9\tau_B$, and $t_6 = 3.0\tau_B$.

$\bar{\rho}(t) = 1/R_{max}(t) \int_0^{R_{max}(t)} dr\rho(r, t)$, where R_{max} is defined by $V_{ext}(r = R_{max}(t)) = 10k_BT$.

The results are tested against Brownian dynamics simulations [29] performed on the same level of accuracy of the diffusion tensor, in which the hard interaction is approximated by a slightly softened one:

$$\frac{v_2(r)}{k_BT} = \begin{cases} [(\frac{\sigma}{r})^{48} - (\frac{\sigma}{r})^{24} + \frac{1}{4}] & \text{if } r \le 2^{1/24}\sigma \\ 0 & \text{else} \end{cases}. \quad (5)$$

In all simulations we chose a finite simulation time step of $\Delta t = 10^{-4}\tau_B$. In order to obtain the time-dependent density $\rho(r, t)$ we perform a large number of $N_{run} = 10^4$ independent runs with different initial configurations sampled from a situation with a static external potential, i.e., Eq. (4) at $t = 0$. Additionally, the densities are compared to those obtained by standard DDFT where hydrodynamic interactions are ignored, i.e., $\boldsymbol{\omega}_{11} = \boldsymbol{\omega}_{12} = 0$. Henceforth, we label the situation including hydrodynamic interactions (H) and the situation where they are neglected (N), respectively. The initial density profile is the equilibrium one for $V_{ext}(r, t = 0)$. Typical simulation snapshots are shown in Fig. 1.

The resulting steady-state of the dynamical density profiles, i.e., the driven breathing mode after initial relaxation, is depicted in Fig. 2 for both cases (H) and (N). The relaxation process itself is presented for the central density field $\rho(r = 0, t)$ and the second moment of the breathing mode $m_2(t) = \int d\mathbf{r} r^2 \rho(r, t)$ in Fig. 3. First of all, theory and simulation results are in very good agreement for both situations (H) and (N) but we observe distinct qualitative differences in the breathing mode: Hydrodynamic interactions tend to damp the density response considerably. The damping is also evident in the much slower oscillation amplitude of the second moment in Fig. 3. The damping effects seen here are caused by the overall motion of the breathing mode which hinders collective streaming due to the counter motion in the opposed part of the trap. Second, as revealed in Figs. 2(a) and 3, the central trap density exhibits a striking nonmonotonic behavior upon expansion with a doubled peak which is solely caused by hydrody-

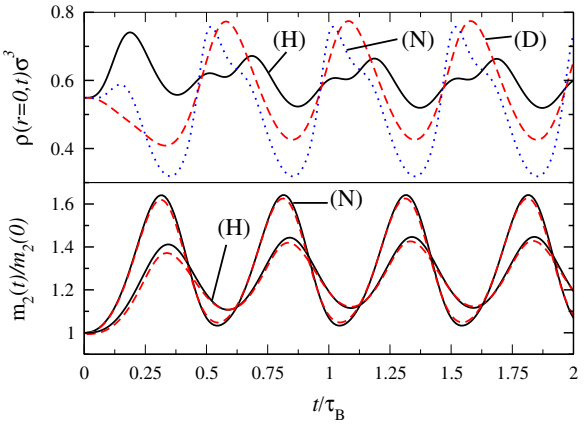

FIG. 3 (color online). Top: Oscillations in the center of the system versus time. DDFT results with hydrodynamic interactions taken into account (H), being neglected (N), and taken into account via a density dependent diffusion coefficient (D). Bottom: Second moment of the breathing mode, $m_2(t)$, versus time t. DDFT (solid curves) and BD (dashed curves) with labeling as before.

namic interactions. This effect is arising from a nontrivial combination of density fluctuations in the neighborhood of the trap center with hydrodynamics: If due to fluctuations more colloids are in one half of the cavity, these will draw strongly to their side the other particles via the trap origin. The averaged net effect leads to a transient density increase at the trap center, as shown in Fig. 3. Finally, the second moment of the breathing mode is slightly off-phase with respect to the driving external potential $\sim \cos(2\pi t/\tau)$, and the hydrodynamic interactions lead to a stronger phase-shifting. The relaxation time towards the steady-state breathing mode is considerably larger for hydrodynamic interactions as compared to the simple Brownian case where the relaxation is almost instantaneous. Additionally we display results obtained when hydrodynamic interactions are incorporated with a D_0 depending on the local density as proposed in [11], labeled (D); see Fig. 3. This indeed improves the results compared to (N) but the oscillations in the center are only slightly damped and do not show a double peaked time evolution in the center.

In conclusion, we have proposed a dynamical density functional theory which includes hydrodynamic interactions between the colloidal particles and applied it to access the driven breathing mode in oscillating optical traps. The theory was confirmed by Brownian dynamics computer simulations. Hydrodynamic interactions were found to damp the response to the driving trap, to increase the relaxation time towards the steady state and to increase the phase shift. Furthermore, a striking double peak in the central trap density was caused by hydrodynamic interactions. These predictions can in principle be tested by real-space experiments on confined colloidal particles. The theory is applicable to a variety of problems in colloidal physics. These include colloidal phase separation, sedimentation and filtration [30], particles in oscillatory shear flow, a microscopic understanding of laser tweezer microrheology [31], and the dynamics of rodlike particles [32,33] both passive and self-propelled. We expect that the qualitative conclusions drawn from the oscillating trap case here are applicable also to oscillatory shear and sedimentation situations.

We thank G. Nägele, S. van Teeffelen, and P. Royall for helpful discussions. This work is supported by the DFG within SFB TR6 (project D3) and by the Graduiertenförderung of the University of Düsseldorf.

*rexm@thphy.uni-duesseldorf.de

[1] H. R. Ma *et al.*, Adv. Phys. **52**, 343 (2003).
[2] F. Sciortino and P. Tartaglia, Adv. Phys. **54**, 471 (2005).
[3] C. Lutz *et al.*, Europhys. Lett. **74**, 719 (2006).
[4] A. Banchio *et al.*, Phys. Rev. Lett. **96**, 138303 (2006).
[5] J. T. Padding and A. A. Louis, Phys. Rev. Lett. **93**, 220601 (2004).
[6] E. Kuusela *et al.*, Phys. Rev. Lett. **90**, 094502 (2003).
[7] G. Nägele *et al.*, J. Chem. Phys. **108**, 9566 (1998).
[8] G. Nägele *et al.*, J. Chem. Phys. **108**, 9893 (1998).
[9] G. Nägele *et al.*, J. Chem. Phys. **110**, 7037 (1999).
[10] B. Cichocki *et al.*, J. Chem. Phys. **117**, 1231 (2002).
[11] C. P. Royall *et al.*, Phys. Rev. Lett. **98**, 188304 (2007).
[12] A. J. Archer and R. Evans, J. Chem. Phys. **121**, 4246 (2004).
[13] U. M. B. Marconi and P. Tarazona, J. Chem. Phys. **110**, 8032 (1999); J. Phys. Condens. Matter **12**, A413 (2000).
[14] S. Henderson *et al.*, Phys. Rev. Lett. **88**, 088302 (2002).
[15] S. Martin *et al.*, Phys. Rev. Lett. **97**, 248301 (2006).
[16] A. Griffin *et al.*, Phys. Rev. Lett. **78**, 1838 (1997).
[17] A. Melzer, Phys. Rev. E **67**, 016411 (2003).
[18] G. Guidarelli *et al.*, Ultrasonics **36**, 467 (1998).
[19] A. J. Archer, J. Phys. Condens. Matter **18**, 5617 (2006).
[20] S. Kim and S. J. Karrila, *Microhydrodynamics: Principles and Selected Applications* (Butterworth-Heinemann, Boston, 1991).
[21] R. Evans, Adv. Phys. **28**, 143 (1979).
[22] J. P. Hansen and I. R. MacDonald, *Theory of Simple Liquids* (Academic, London, 2006), 3rd ed..
[23] S. Dietrich and A. Haase, Phys. Rep. **260**, 1 (1995).
[24] B. Götzelmann *et al.*, Phys. Rev. E **53**, 3456 (1996).
[25] A. Trokhymchuk *et al.*, J. Chem. Phys. **123**, 024501 (2005).
[26] Y. Rosenfeld, Phys. Rev. Lett. **63**, 980 (1989).
[27] A. González *et al.*, Phys. Rev. Lett. **79**, 2466 (1997).
[28] J. Rotne and S. Prager, J. Chem. Phys. **50**, 4831 (1969).
[29] *Computer Simulation of Liquids*, edited by M. P. Allen and D. J. Tildesley (Clarendon Press Oxford, Oxford, 1989).
[30] A. P. Philipse, Curr. Opin. Colloid and Interface Sci. **2**, 200 (1997).
[31] A. Meyer *et al.*, J. Rheol. (N.Y.) **50**, 77 (2006).
[32] M. Rex *et al.*, Phys. Rev. E **76**, 021403 (2007).
[33] M. Bier and R. van Roij, Phys. Rev. E **76**, 021405 (2007).
[34] See EPAPS Document No. E-PRLTAO-101-066840 for movies of the time evolution of $\rho(\mathbf{r}, t)$ and typical simulation runs for both setups (H) and (N). For more information on EPAPS, see http://www.aip.org/pubservs/epaps.html.